FINAL TECHNICAL REPORT

NASA Grant NSG - 1651

# Holographic Fabrication of Gratings in Metal Substrates

Report Period

November 1, 1981 - October 31, 1982

by

R. M. Fletcher, D. K. Wagner and J. M. Ballantyne

School of Electrical Engineering
Cornell University
Ithaca, NY 14853

CONTENTS

# I. INTRODUCTION

There are many investigations currently underway in the study of materials suitable for solar cell applications. Some of the more esoteric studies involve the use of an inexpensive foreign substrate as a supporting structure for the active solar cell device. Such a structure is especially desirable for gallium arsenide, a relatively efficient and expensive solar cell material. Unfortunately, gallium arsenide grown on a foreign substrate is typically fine-grained polycrystalline and not well-suited for high efficiency solar cells. There are techniques, however, which show promise in achieving larger grain growth and hence higher cell performance.

This report describes a program for investigating the grain enlargement resulting from the laser recrystallization of a thin gallium arsenide film on a patterned substrate, a technique known as graphoepitaxy.[1] More specifically, the effects of recrystallizing an uncapped gallium arsenide film using a c.w. Nd:YAG laser operating at 1.06 μm were studied. In an effort to minimize arsenic loss from the film, the specimens were held in an arsine atmosphere during recrystallization.

In the course of this work, two methods for fabricating patterned substrates were developed--one using reactive ion etching of a molybdenum film on both sapphire and silicon substrates and another by preferential wet etching of a silicon substrate onto which a film of molybdenum was subsequently deposited. The need for the molybdenum film in both cases was to provide a surface on which the gallium arsenide could be successfully grown.

What follows is a description of the laser recrystallization system constructed specifically for this project and a description of the substrates fabricated for the recrystallization process. The results of the laser recrystallization are then presented.

## II. LASER RECRYSTALLIZATION SYSTEM

In the design and construction of the laser system several considerations were of importance. First, since a c.w. laser was to be used, sufficient power in the beam was necessary to assure melting of the GaAs film under various conditions of substrate temperature and scanning speed. A Control Laser Corporation model 2660 100W c.w. Nd:YAG laser was selected as suitable for this task.

Second, the specimen had to be contained in a sealed cell into which arsine or some inert gas could be introduced. Figure 1 illustrates the cell that was constructed. The cell is a machined stainless steel cylinder with a BK-7 glass window assembly mounted at one end and a heated pedestal mounted at the other end. A molybdenum plate brazed to the top of the pedestal provides a surface for attaching the specimens to the pedestal using melted indium as an "adhesive". Good thermal contact is thus achieved. Cartridge heaters inserted into the pedestal are capable of providing substrate temperatures up to 600$^{o}$C. A thermocouple in the pedestal is used to monitor the temperature. The upper window assembly of the cell is removable, providing access to the pedestal for specimen placement. "O"-ring seals at all the cell joints assure a leak-tight system and permit control of the internal cell atmosphere through the gas ports on the sides of the cell.

Because arsine cracks into arsenic vapor and hydrogen when heated during recrystallization, arsenic lends to condense on the cool inner surface of the cell window. To prevent obstruction of the laser beam by the

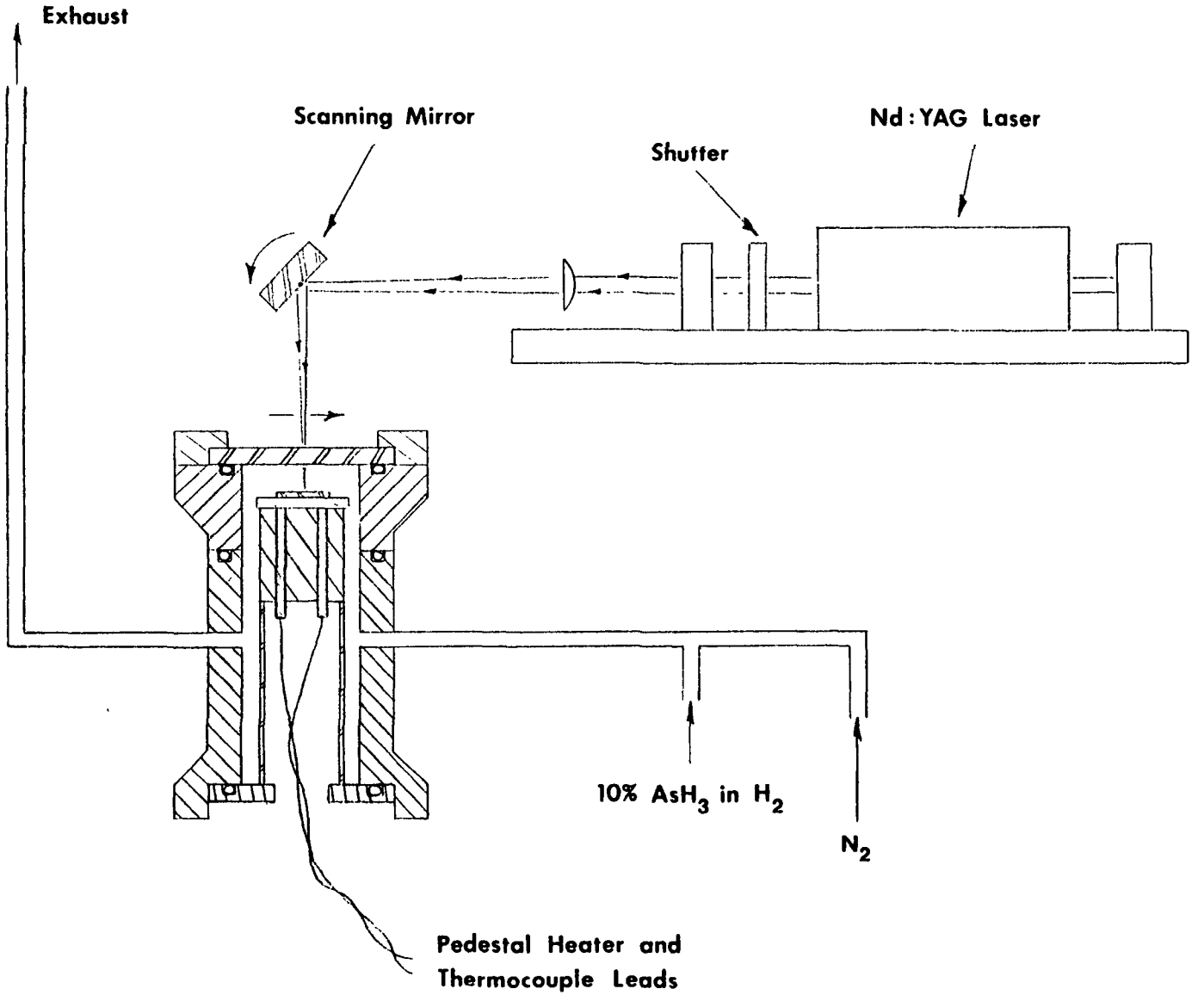


Figure 1. Diagram of the scanning system. The recrystallization cell is shown with a specimen on top of the heated pedestal. An arsine-hydrogen mixture or nitrogen can be introduced into the cell. Focused light from the laser is directed onto the specimen by the scanning mirror.

arsenic film, a second window assembly had to be constructed. This assembly consists of a sapphire window brazed to a metal flange which is wrapped with nichrome wire. Resistance heating of the flange and window up to 400°C slows the arsenic deposition and allows sufficient time for recrystallization before the window begins to collect an appreciable arsenic film.

Also diagrammed in Figure 1 are a focussing lens and a scanning mirror. The lens can be either a cylindrical lens for producing a roughly rectangular focussed spot or a spherical lens for a circular spot. The focussed dimension is ~70 μm for both types of lenses. The unfocussed dimension for the cylindrical lens depends on the diameter of the beam emerging from the laser. Selectable intra-cavity laser aperatures provide beam sizes ranging from 2.5 mm to a maximum of 6 mm, the larger aperatures allowing greater maximum laser power up to 100 W. Higher light intensities were achievable with the spherical lenses which were used most of the time. The scanning mirror is mounted to a closed-loop galvanometer motor (General Scanning model G-300PD). A ramp signal applied to the motor provides scanning of the beam along one axis with speeds ranging from $<1.0$ cm $s^{-1}$ to 100 cm $s^{-1}$. Additional circuitry controls the opening and closing of the laser shutter at the appropriate times. The cell is mounted on a translation stage for motion of the specimen along the axis perpendicular to the scan direction. Described briefly (see Figure 2), when the scan cycle is initiated, the laser shutter automatically opens, and the mirror makes a scan at some pre-set velocity. Upon completion of a single scan the shutter closes, and the mirror returns to its original position. More scans can then be made over the same area, or the cell can be translated to scan another region of the specimen. Figure 3 is a photograph of the scanning system.

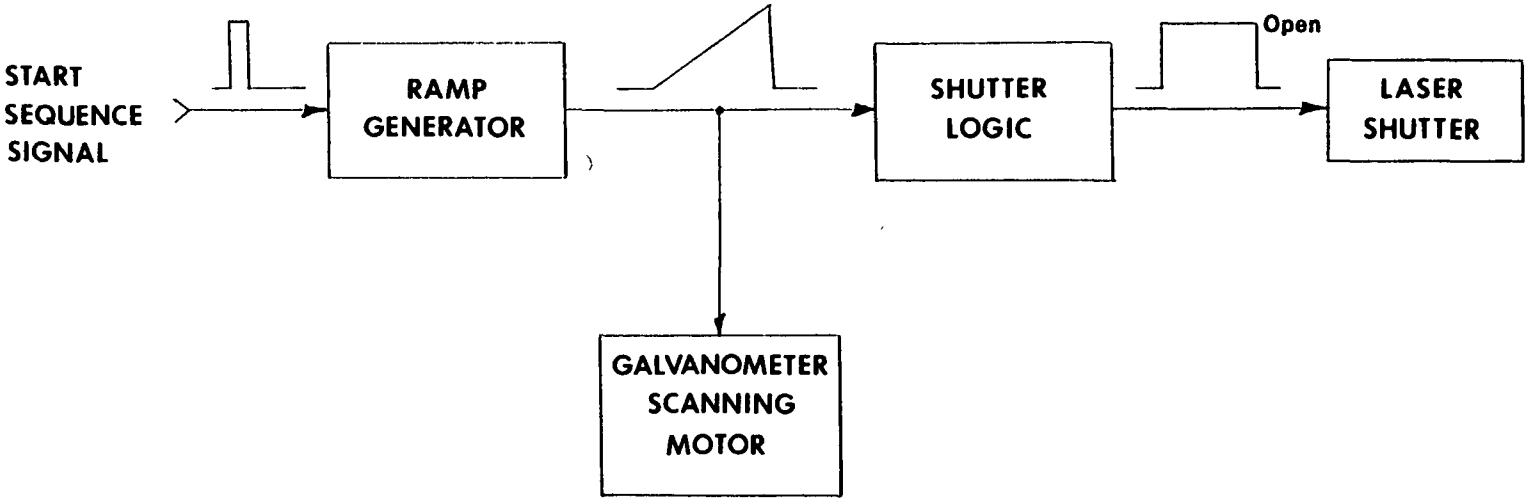


Figure 2. A block diagram of the scanning electronics. A start signal initiates a linear ramp and opens the laser shutter. The ramp drives the scanning mirror, and at its peak the shutter closes and the mirror returns to its initial position.

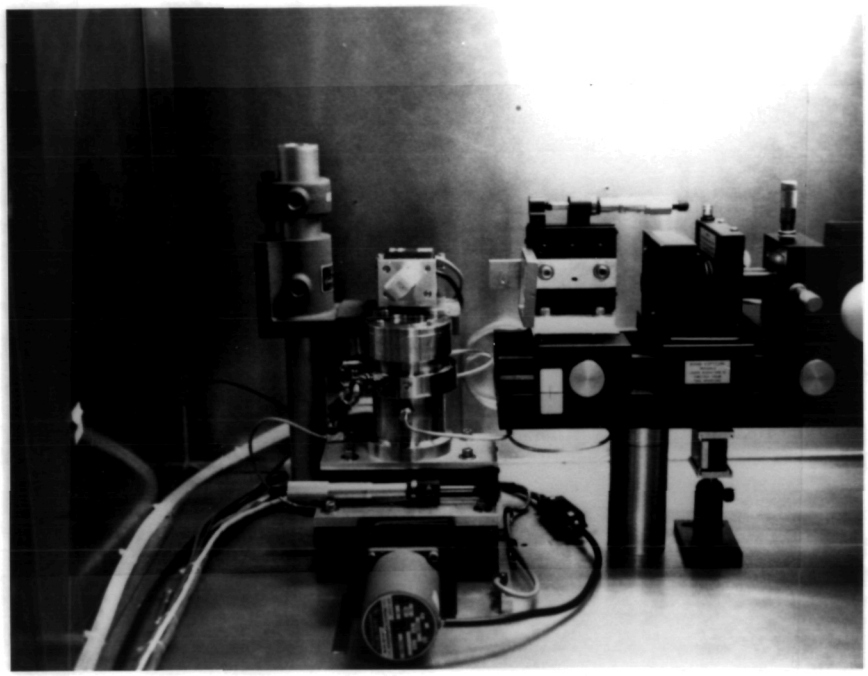

Figure 3. Photograph of the recrystallization system. The specimen cell, mounted on top of a translation stage, is located in the center of the photo. The scanning mirror can be seen just above the cell. To the right are the focussing lens and the Nd:YAG laser.

The laser, scanning optics, and specimen cell, as well as the gas handling manifold and arsine tank, are contained in a vented steel cabinet. The purpose of this cabinet is two-fold, as it provides containment for the intense laser light and acts as a safety exhaust hood in the event of an accidental arsine leak. In addition, rather than simply exhaust the arsine to the outside, a cracking furnace located down-line from the specimen cell assures complete cracking of the arsine. The resulting hydrogen gas is exhausted, and the arsenic is collected in a filter for proper disposal.

## III. SUBSTRATE PREPARATION

An essential part of graphoepitaxy is the preparation of the patterned substrates. The first substrates fabricated for this project were produced with NASA support under grant number NSG 1651[2]. These substrates consisted of a sapphire or silicon wafer onto which a film of molybdenum was e-beam evaporated. Using photolithographic masking techniques to define the grating patterns the molybdenum film was etched by reactive ion etching (R.I.E.). The result (see Figure 4) was an array of four 1mm square grating patterns of differing periods: 2 μm, 4 μm, 8 μm, and 16 μm. GaAs was then grown on the patterned molybdenum by MBE (at Cornell) or MOCVD (at NASA Langley).

There were several problems associated with these substrates. First, all the sapphire substrates fractured catastrophically when subjected to the laser scanning, apparently due to the thermal stress from intense local heating of the GaAs and molybdenum films. Changing to a silicon substrate reduced the occurrence of fracturing substantially but did not

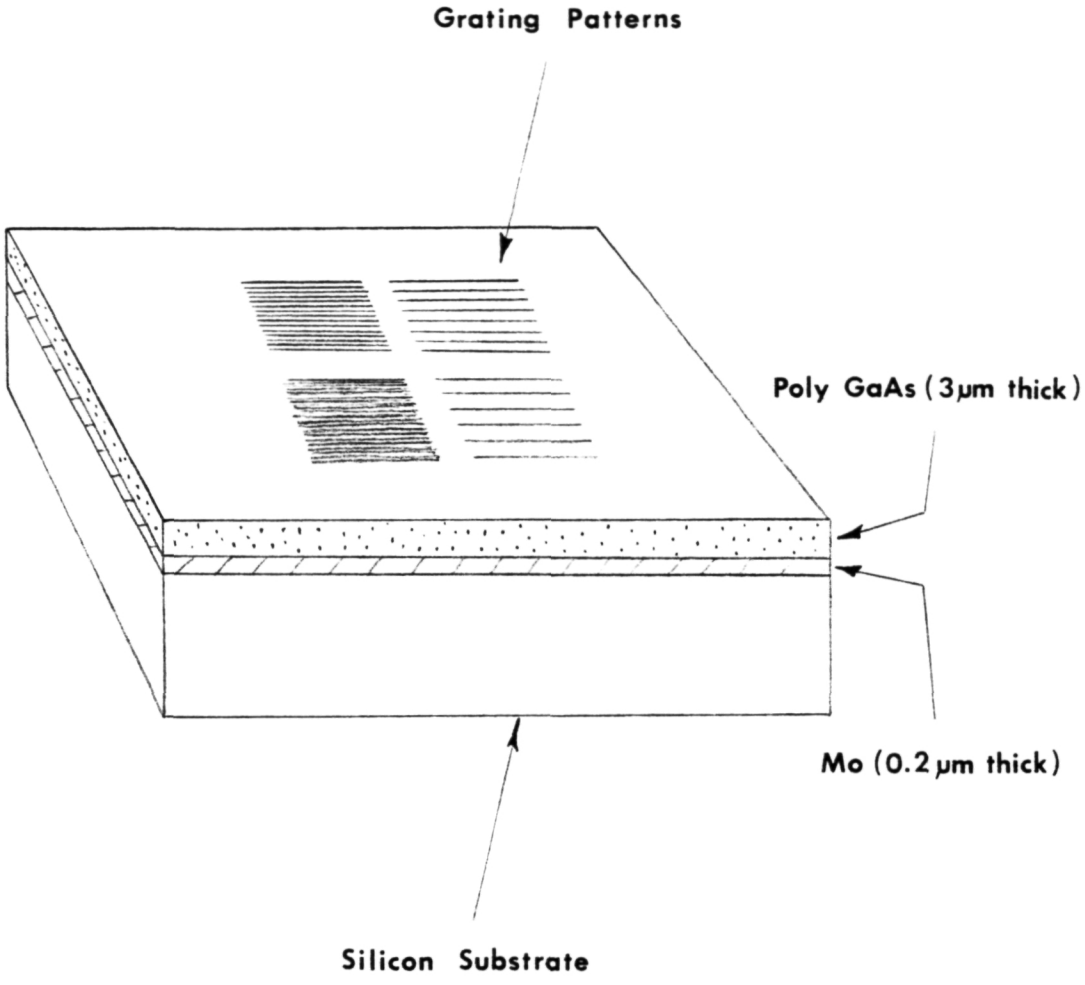


Figure 4. Specimen geometry. A 0.2 μm film of molybdenum is electron-beam evaporated onto a silicon substrate. After etching a grating pattern in the molybdenum, a layer of fine-grained polycrystalline GaAs is grown on top by MBE or MOCVD.

eliminate it completely. The superior thermal conductivity of silicon over sapphire, by roughly a factor of 10, is probably the reason for the difference in fracturing.

Another problem with the R.I.E. gratings was the surface roughness of the sidewalls and bottoms of the grooves. Apparently because of this roughness the laser recrystallization produced little, if any, improvement in the GaAs film.

Finally, because of the complexities of the fabrication process and the inconsistencies of the equipment used (especially the reactive ion etcher), it was difficult to produce the grating patterns in sufficient quantities. Uniform grating patterns of sufficient area to facilitate the laser scanning process were also difficult to produce.

Owing to the combination of all these problems another approach to the grating fabrication was taken. As suggested by reports on the anisotropic etching of silicon, it is reasonably simple to obtain large area grating patterns by preferential wet etching techniques.[3] We were able to produce "V"-groove-type grating patterns in (100) silicon wafers using these techniques. SEM photographs of some of the 5 μm and 20 μm period patterns are shown in Figure 5. The oxide mask is clearly present in both photographs. The depth of the grooves is ~ 1 μm.

Larger grating areas were obtained by using the same photolithography mask as was used for the R.I.E. gratings but using a projection mask aligner having a smaller reduction ratio (4:1 as opposed to 10:1). The result was an array of four 2.5 mm square patterns having periods of 5 μm, 10 μm, 20 μm, 40 μm. The effect of larger period gratings was not felt to be of major concern at this stage when compared to the advantage of larger grating area.

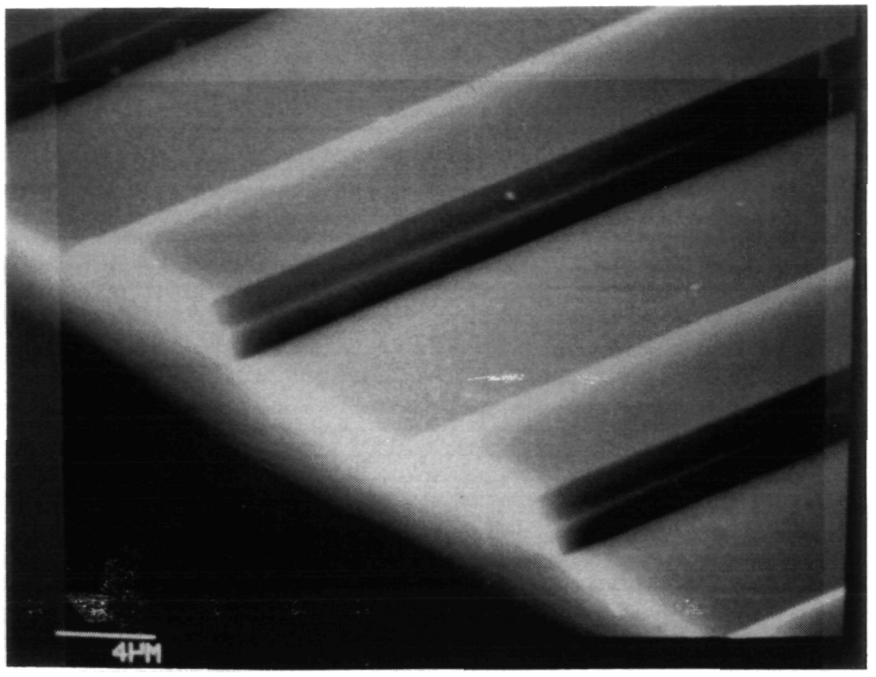


(a)

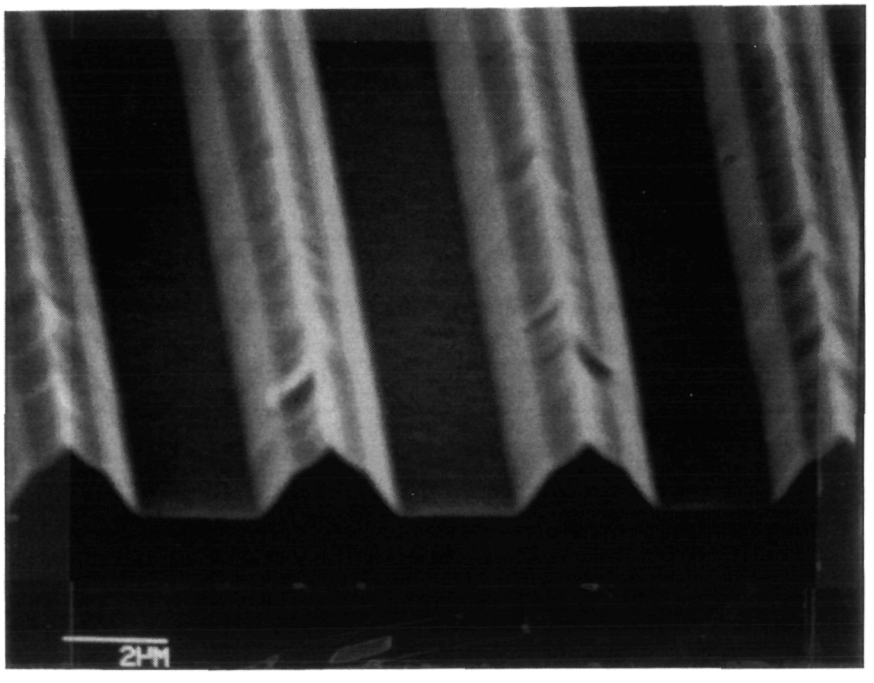


(b)

Figure 5. SEM micrographs of preferentially etched grooves on silicon with the oxide mask still present. (a) 20 μm period grating. (b) 5 μm period grating. The sidewalls of the grooves are (111) planes and make an angle of $54.74^{o}$ with the plane of the (100) surface of the wafer.

The basic processing steps for producing successful gratings from a (100) silicon wafer with 1 μm of thermally grown oxide are as follows:

1. Clean silicon wafer with acetone followed by methanol.
2. Etch in 10% buffered HF and D.I. water for 30 s.
3. Rinse with D.I. water for 5 min.
4. Bake at 200°C for 30 min.
5. Remove from oven and immediately soak in HMDS adhesion promoter for 5 min.
6. Spin dry.
7. Spin on AZ 1450-J resist at 6000 rmp.
8. Pre-bake at 100°C for 45 min.
9. Expose wafer to mask.
10. Mid-bake at 100°C for 20 min.
11. Develop in 1:5 Microposit developer and D.I. water at 23°C for 40 s.
12. Post-bake at 120°C for 30 min.
13. Etch oxide mask in buffered HF for 5 min.
14. Strip resist pattern with acetone.
15. Etch silicon in 50% wt. KOH and D.I. water and 5% vol. triethanolamine at 40°C for 30 min.
16. Rinse in D.I. water and remove oxide mask with buffered HF.

The KOH preferential etch solution by itself produces good "V"-groove patterns with smooth sidewalls if allowed to etch a complete "V". Since our interest was in a flat bottomed groove the addition of triethanolamine[4] to the KOH solution helped to improve the smoothness of the groove bottoms, as illustrated in Figure 6.

The final step before the GaAs growth was the application of a molybdenum film to the patterned silicon. This step was easily accomplished by e-beam evaporation of a film on the order of 2000 Å thick. Both the uniformity and adhesion of the molybdenum on the silicon were excellent.

Growth of the GaAs films was carried out in the Cornell MOCVD system. The first attempt was not successful because the trimethylgallium bubbler source ran dry at the beginning of the growth run. Therefore, what was supposed to be a 3 μm thick film of continuous polycrystalline GaAs turned out to be scattered nucleation islands of GaAs. The results are pictured

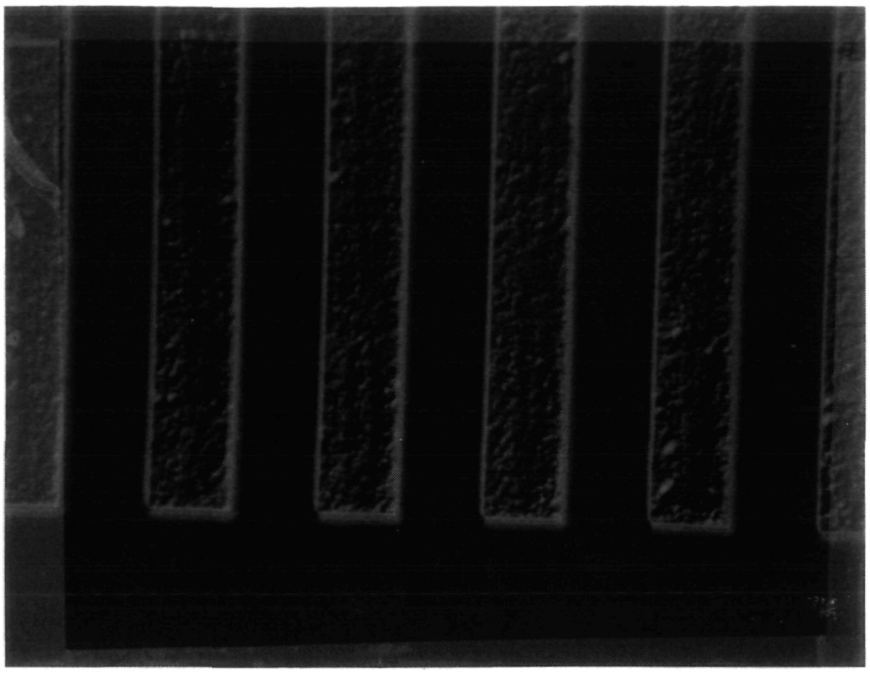

(a)

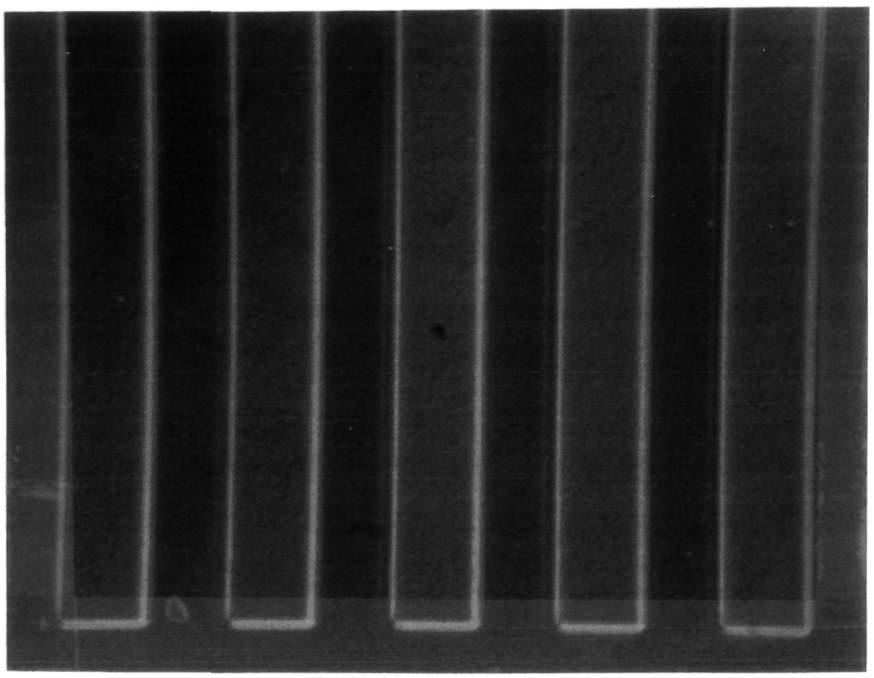

(b)

Figure 6. Optical Nomarski micrographs of the etched grooves in silicon at 500X. (a) Etched in 50% wt. KOH and water. (b) Triethanolamine added to etch solution (5% vol.) to improve smoothness of groove bottom.

in Figure 7 which shows randomly scattered growth outside the 40 μm period grating area and highly controlled growth along the edges of the grating grooves, with strong preference given to the lower edges of the grooves. In addition, the area immediately outside the grating lines is depleted of growth for a characteristic distance of about 20 μm. The 5 μm period grating shows an almost even distribution of growth within the groove area. The nuclei are smaller, but they still appear to grow on the walls of the grooves and then up over the lines. The growth effects observed here could, with further investigation, indicate preferential orientation occurring under the influence of the grating during the initial stages of growth. In addition, this effect could be of some use in the study of growth and nucleation kinetics of MOCVD.

After this unsuccessful attempt at growing a GaAs layer, the substrates were cleaned of the GaAs nuclei by etching in an ammonia-hydrogen peroxide solution. The molybdenum film was undamaged, and the substrates were prepared for another MOCVD run. The growth temperature during this run was 650$^{o}$C, and a 3 μm thick film was successfully grown. Three separate wafers were thus obtained with the four-grating pattern reproduced nine times on each wafer.

The growth of the GaAs in the grating areas was not complete for all the patterns on two of the wafers. The third wafer achieved excellent coverage over the entire surface, however, All three wafers showed evidence of some cracking and peeling of the GaAs film at the edges. Adhesion of the GaAs to the grating areas seemed to be adequate. Each of the three wafers was sawn into nine pieces, each piece containing the four-grating

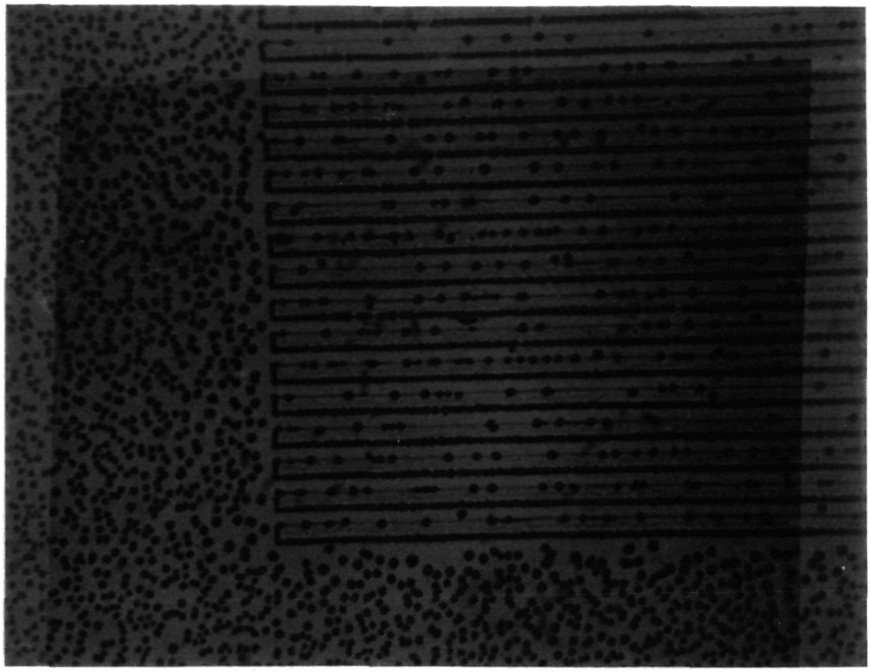

(a)

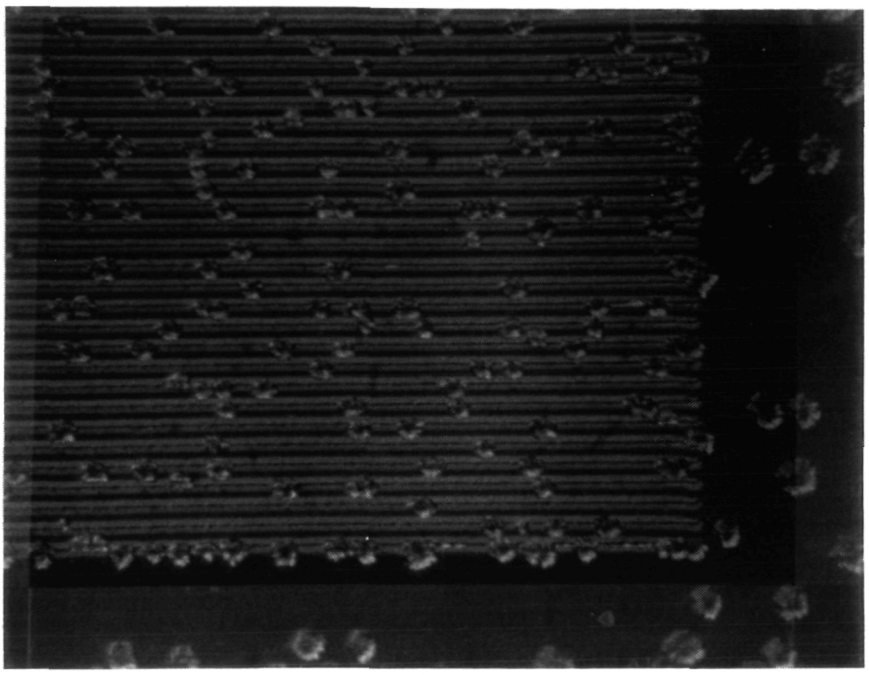

(b)

Figure 7. Onset of GaAs nucleation from an unsuccessful MOCVD growth run. (a) 40 μm grating at 100X. (b) 5 μm grating at 500X.

pattern. Flaking of the GaAs film during sawing was minimal and limited to the edges of the pieces; the grating areas remained intact.

## IV. LASER RECRYSTALLIZATION

Initial laser scans were performed on unpatterned GaAs films in order to determine the range of values of laser power, scan speed, and substrate temperature necessary for melting and recrystallization of the film to occur. Because GaAs is transparent at room temperature to the 1.06 μm laser light, it was immediately necessary to raise the substrate temperature to increase the optical absorption by shrinkage of the bandgap energy. For single crystal GaAs the bandgap energy at ~ 535°C is comparable to the 1.06 μm photon energy. We found that raising the substrates to ~ 570°C produced sufficient optical absorption for melting of the GaAs film to occur. A slight reduction of the temperature meant that considerably more laser power was needed to achieve comparable effects in the film.

At a laser power of ~ 20 W ($2.5 \times 10^5$ W cm$^{-2}$) and a scan speed of 1.5 cm s$^{-1}$ there was no effect on the GaAs film other than a slight lightening in color from the as-grown dull gray. This lightening effect was unobservable under microscopic examination, and no structural change in the film was seen. By increasing the laser power or by reducing the scan speed, a threshold was achieved where the film began to show definite melting effects.

In Figure 8 are optical microphotographs at 200X and 500X showing the results of a single scan made over a 3 μm GaAs film grown on an unpatterned substrate. This particular example demonstrates several effects commonly observed. The most striking feature is the lack of adhesion of the GaAs to the underlying molybdenum, which allows the melted GaAs to coalesce and ball-up due to surface tension. What remains of the GaAs film, however

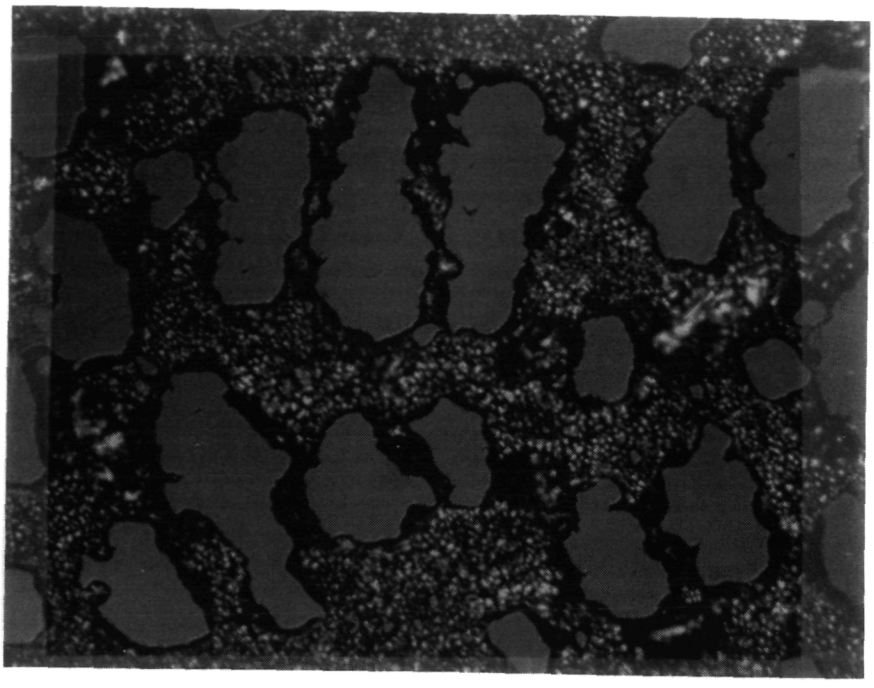

(a)

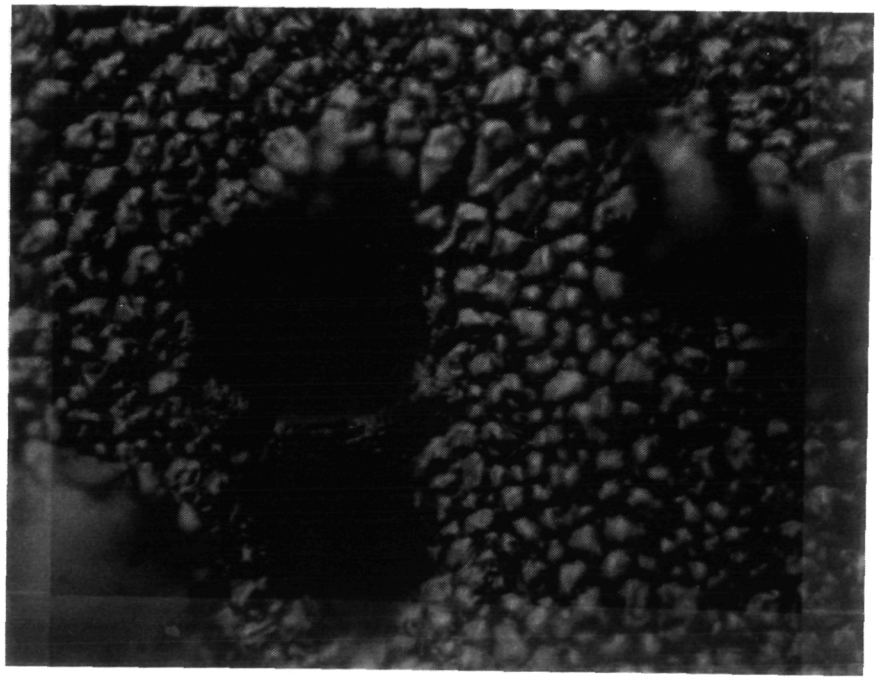

(b)

Figure 8. Laser recrystallized GaAs film on an unpatterned substrate showing problems with adhesion to the molybdenum. (a) 200X. (b) 500X. Laser power: 38 W ($4.8 \times 10^5$ W $cm^{-2}$); Scan speed: 1.0 cm $s^{-1}$.

shows the granular appearance of slight grain enlargement to about 10 μm. This scan was made at a laser power of 38 W ($4.8 \times 10^5$ W $cm^{-2}$) with a scan speed of 1.0 cm $s^{-1}$. The substrate temperature was 550°C. For comparison, an as-grown GaAs film is shown in Figure 9 at 500X.

From the results of numerous scans it became evident that there is a trade-off between laser power and scan speed which yields similar results. The ratio of laser power to scan speed was kept in a range of 20 to 40 W•s $cm^{-1}$ to obtain the best results. At higher laser power and scan speed, however, more consistent results were obtained with less severe damage to the film occurring at the edges of the specimens due to excessive heating. Laser powers around 80 W and scan speeds around 4.0 cm $s^{-1}$ were commonly used, although a whole range of both parameters was investigated. Changes in laser power and scan speed were made in increments of ~ 5%, small enough so that no special regions of interest would be missed.

After establishing general guidelines for the scan parameters using GaAs films on unpatterned substrates, laser scans were performed on the GaAs films grown on the "V-groove" grating substrates. What follows is a description of the various effects observed.

The most promising results occurred with the 5 μm period gratings. As mentioned previously, adhesion of the GaAs to the molybdenum is poor after growth and during the laser recrystallization process. The presence of the small period grating, however, improves the adhesion considerably. Pictured in Figure 10 are SEM photographs of a 5 μm grating. The left half of Figure 10a shows a laser scanned area; the right half shows an area outside the beam path. The laser power was 38 W ($4.8 \times 10^5$ W $cm^{-2}$), and the scan speed was 1.5 cm $s^{-1}$. The bare patches are regions where

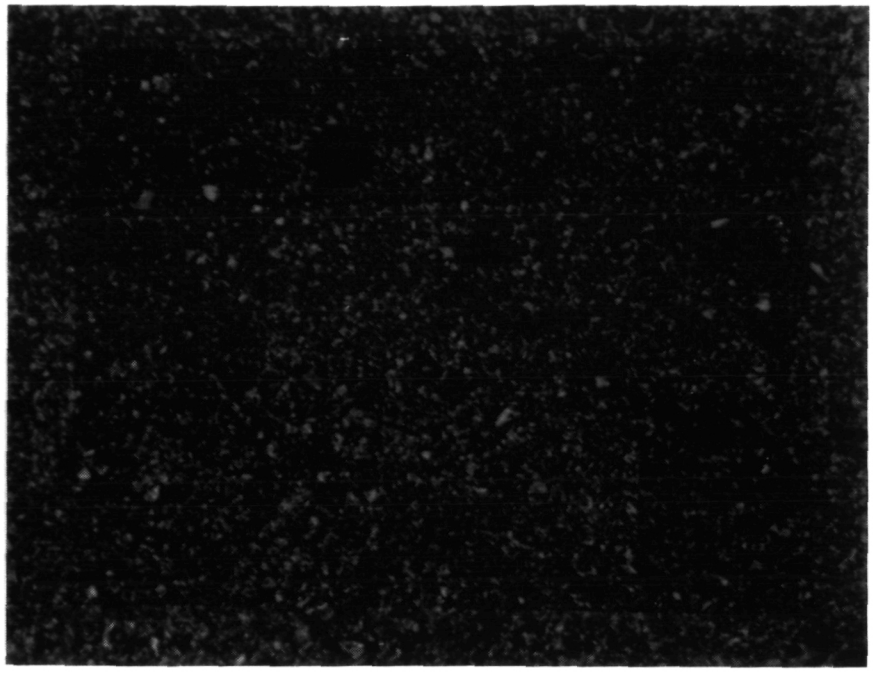

Figure 9. Optical Nomarski micrograph of as-grown GaAs on an unpatterned substrate. Magnification is 500X.

the MOCVD GaAs growth was incomplete. Even at these patches the film has resisted balling-up. Close-up views of the scanned regions are pictured in Figure 10b. Figure 11 shows the as-grown GaAs for comparison.

An interesting feature of the scanned film apparent in Figures 10a and 10b is the presence of globular shapes which tend to line up with the grating. This particular feature is characteristic of all the scans on the 5 μm gratings. Without these globules the film is fairly smooth, when compared to the as-grown film, and there is little evidence of the grating underneath.

It should be noted that the appearance of the recrystallized film is the same whether the specimen cell is filled with arsine or nitrogen, especially with respect to the presence of the globular shapes. This has been found to be the case for all the scans performed to date, an indication that any arsenic loss that may be occurring is too small to affect the gross changes in the film as observed by microscopic examination, or that there is not enough $As_2$ partial pressure in either case to suppress arsenic loss.

On another specimen, with the scan speed reduced to 1.0 cm $s^{-1}$, the recrystallized film appears slightly different, as seen in Figure 12. The globular shapes are less obvious and the film seems to be composed of plate-like patches, with some crystalline structure visible. A scanned region just outside the grating area, seen in Figure 13a, shows no sign of the structure associated with regrowth over the grating. The as-grown film is shown in Figure 13b for comparison. The crack seen in the film in Figure 13a occurred after recrystallization. Such cracks were often observed in the films on unpatterned substrate, but few cracks were found within the grating areas.

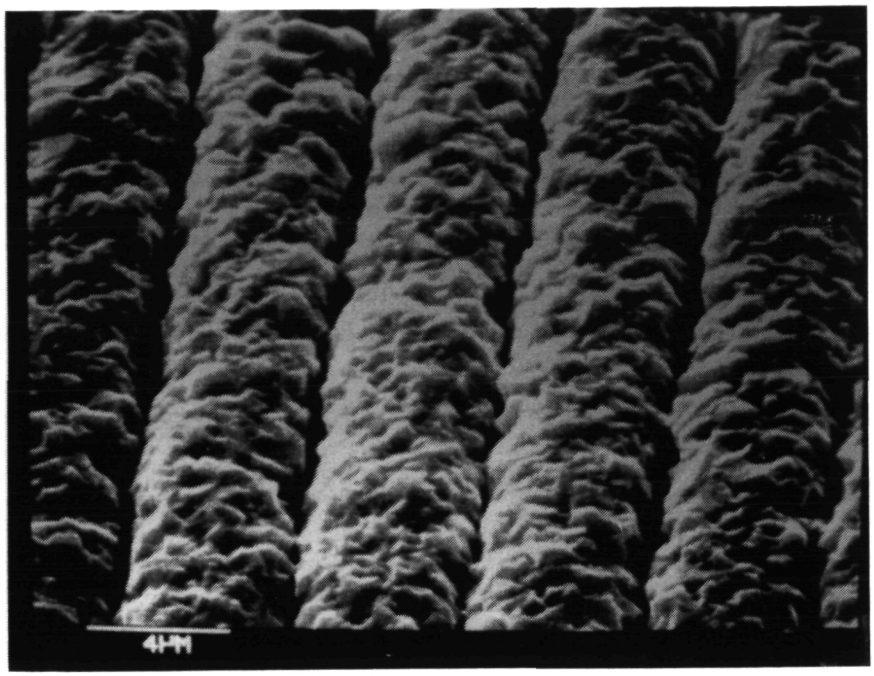

Figure 11. SEM micrograph of as-grown GaAs on a 5 μm grating.

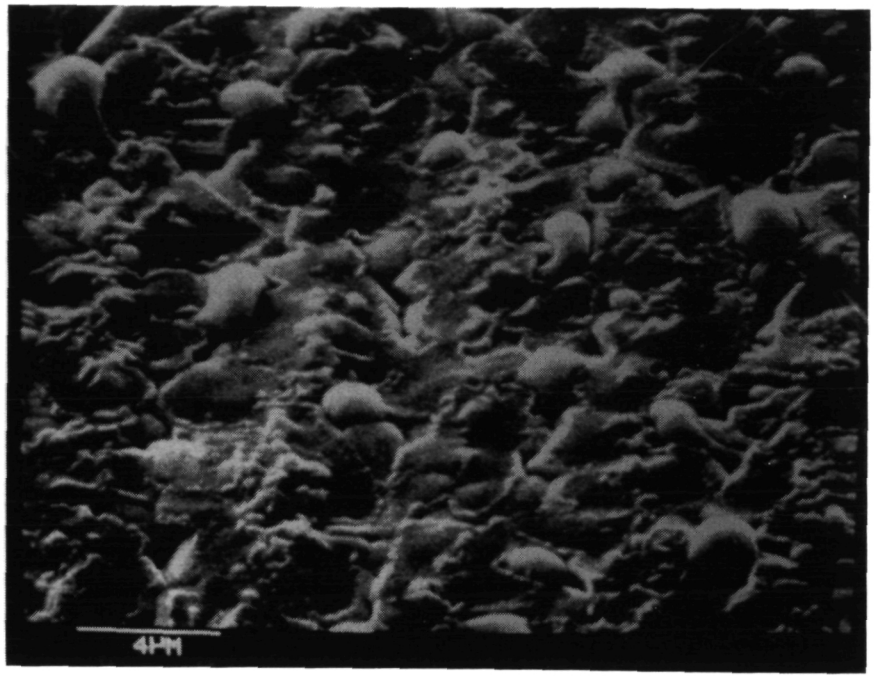


Figure 12. SEM micrograph of a recrystallized 5 μm grating. Laser power: 38 W ($4.8 \times 10^5$ W $cm^{-2}$); Scan speed: 1.0 cm $s^{-1}$.

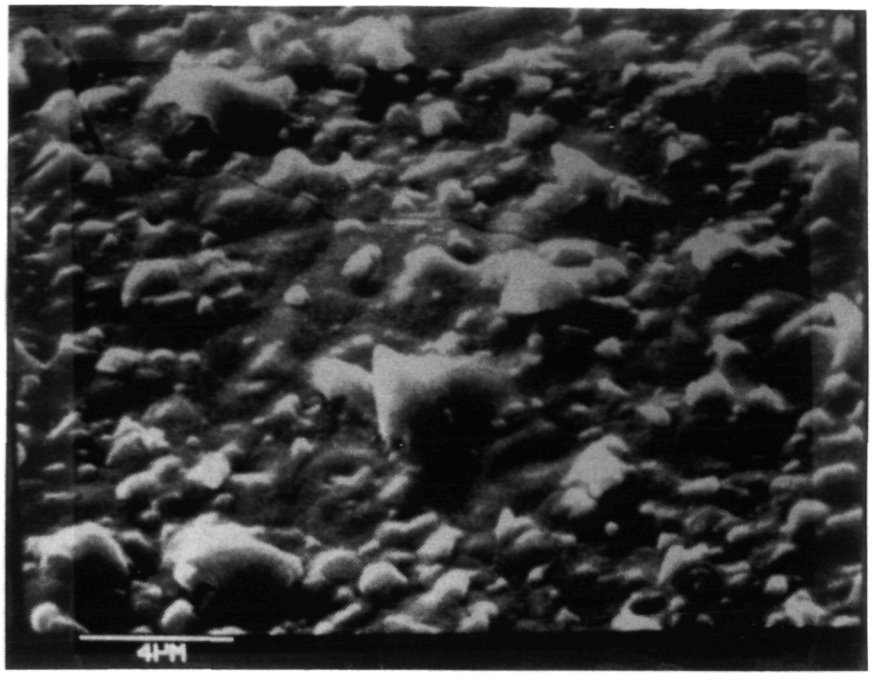


(a)

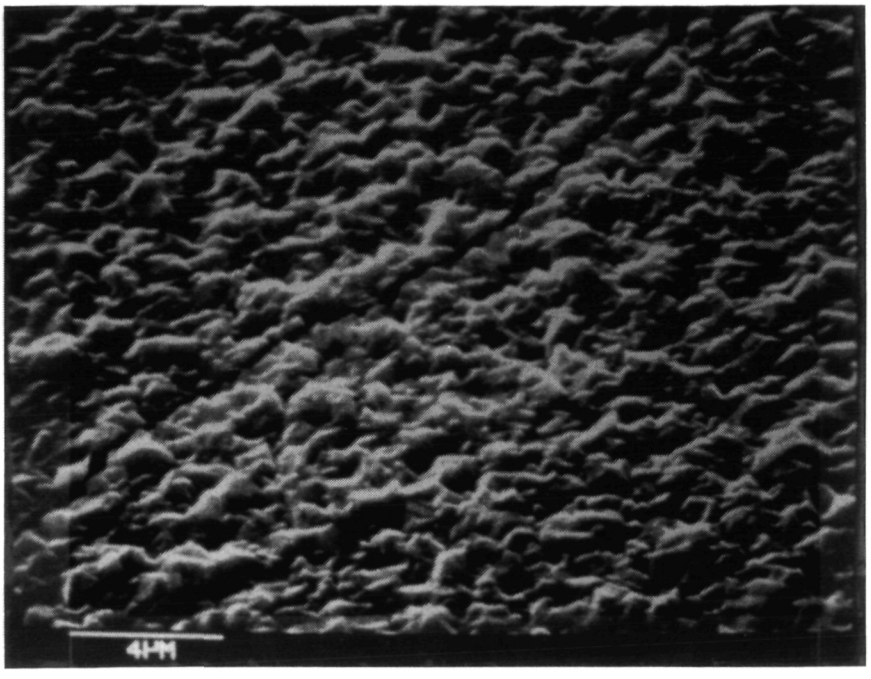


(b)

Figure 13. (a) SEM micrograph of a recrystallized film on an unpatterned area of substrate. Laser power: 38W ($4.8 \times 10^5$ W $cm^{-2}$); Scan speed: 1.0 cm $s^{-1}$ (b) As-grown GaAs film on unpatterned substrate.

As mentioned previously the MOCVD growth was not complete over all the grating areas. Since nucleation begins on the grating lines and then grows out to fill in the grooves, some of the larger period gratings tended to have gaps in the GaAs film at the center of the grooves. The as-grown GaAs film on a 10 μm period grating with this problem is shown in Figure 14. The laser scanned region of this grating is illustrated in the optical micrograph of Figure 15a at 100X. The beam path, clearly evident in the photograph, is scattered with dark patches which are shown magnified in the SEM photo of Figure 15b. When melted by the laser beam, the GaAs sends to "crawl" along the grating lines and coagulate into the droplet shapes shown. Under higher magnification in Figure 16a, the GaAs is seen to adhere to the sidewalls of the grating lines and occasionally form a crystal-shaped "bridge" between the lines. In other cases, (Figure 16b) the film covers the lines more completely forming a triangular-shaped structure that mimicks the "V-groove" shape of the molybdenum covered silicon lines underneath.

When the as-grown film completely covers the 10 μm grating pattern, as in Figure 17a, the recrystallized film also remains largely continuous, although there is still some tendency for the GaAs to crawl out of the grooves (Figure 17b). A high mangification view of this film in Figure 18 reveals features similar to the 5 μm gratings, namely the plate-like crystalline structures and the periodic globular spots.

The 20 μm period gratings show the poor adhesion characteristics of the 10 μm gratings but to a larger degree. The non-continuous as-grown film in Figure 19a recrystallizes to the form seen in Figure 19b. Even when the film is continuous, the GaAs still crawls out of the grooves, as seen in Figure 20a, and much of the material has coalesced into the droplet shapes shown in Figure 20b.

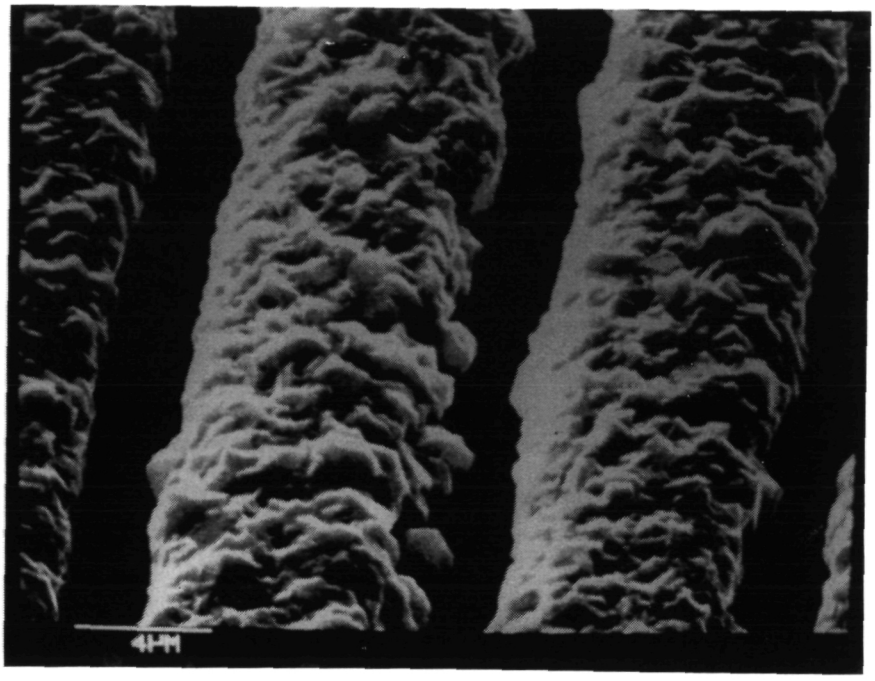

Figure 14. As-grown GaAs film on a 10 μm grating. The gaps between the grating lines are from incomplete MOCVD growth.

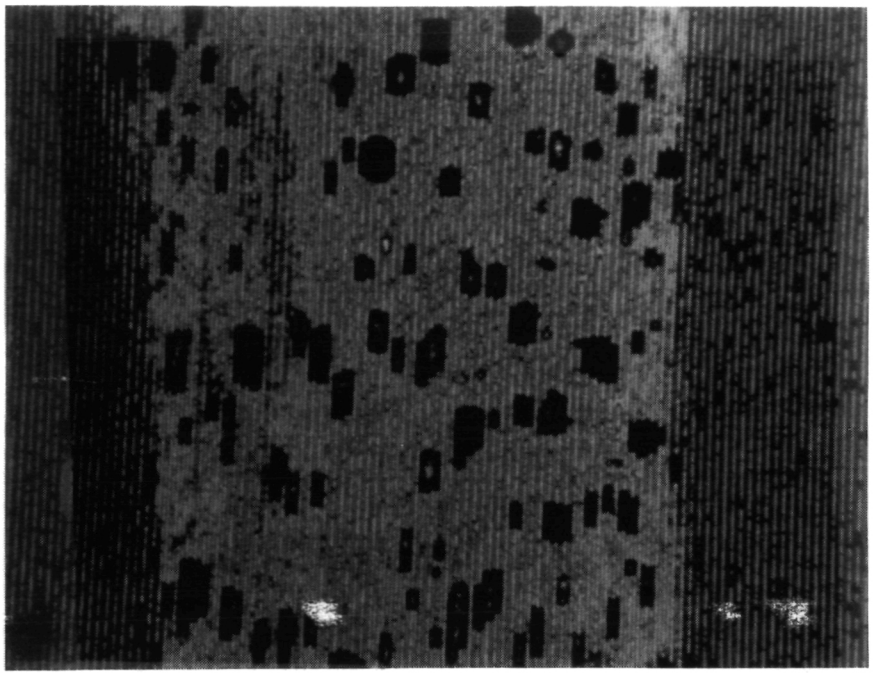

(a)

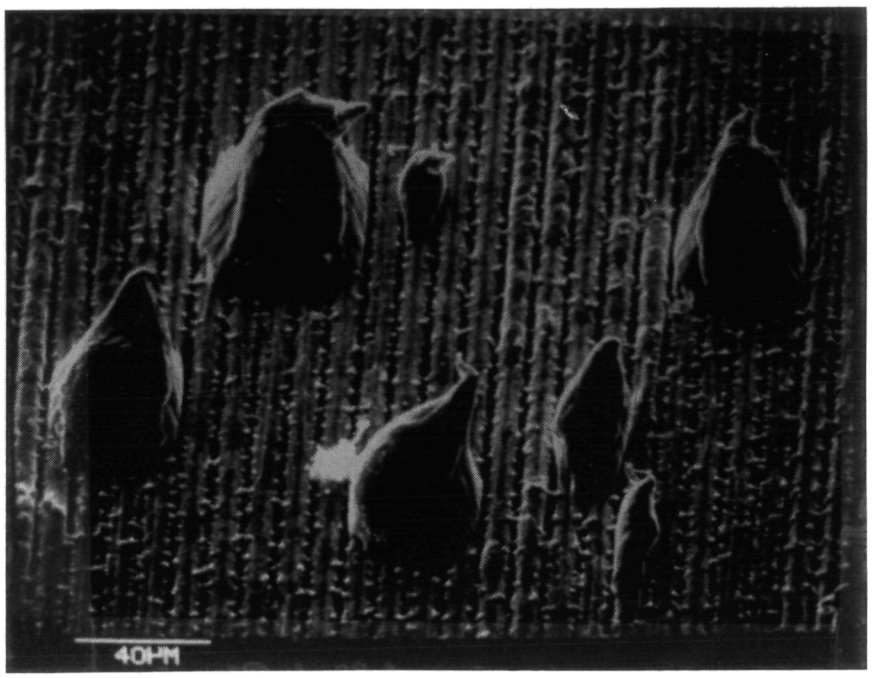


(b)

Figure 15. (a) Optical micrograph of a scanned 10 μm grating at 100X. (b) SEM micrograph of the scanned area showing details of the dark patches.

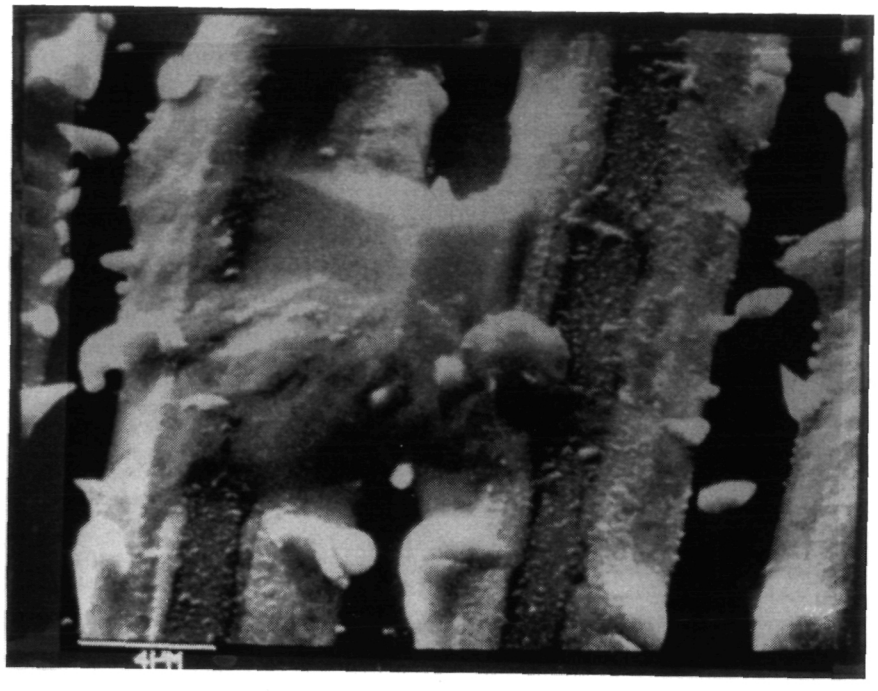

(a)

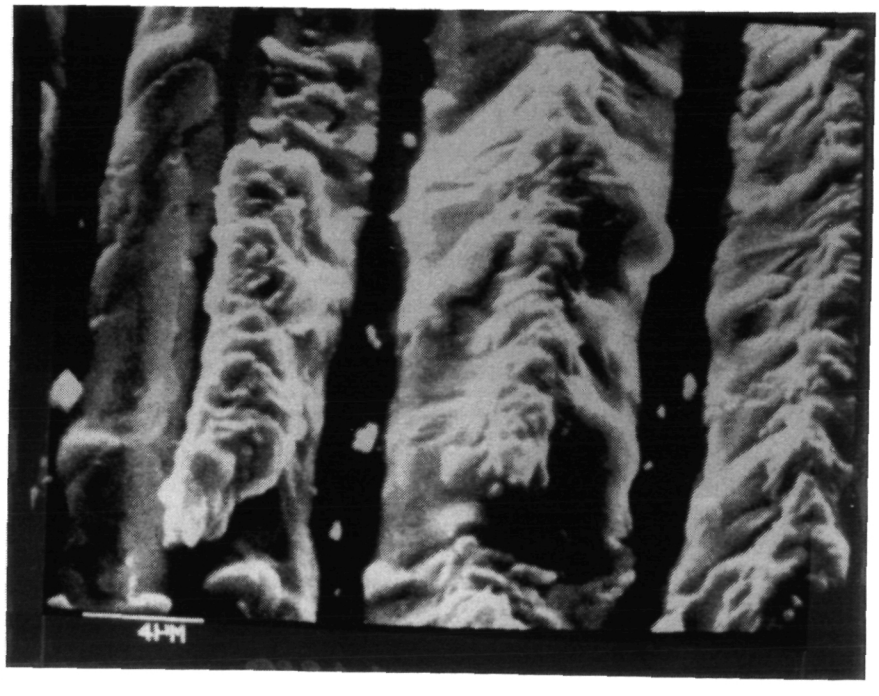

(b)

Figure 16. SEM micrographs of the types of effects observed on the 10 μm gratings. (a) The GaAs has left the tops of the lines but tends to adhere to the sidewalls. Occasionally, crystalline "bridge" structures join the lines. (b) Here the GaAs mostly covers the grating lines in triangular shaped mounds.

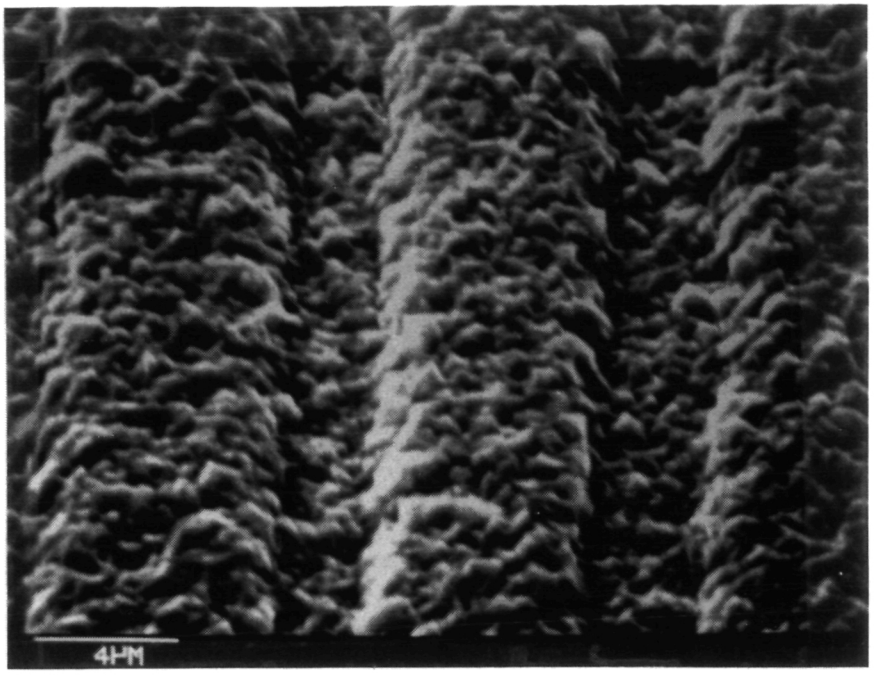


(a)

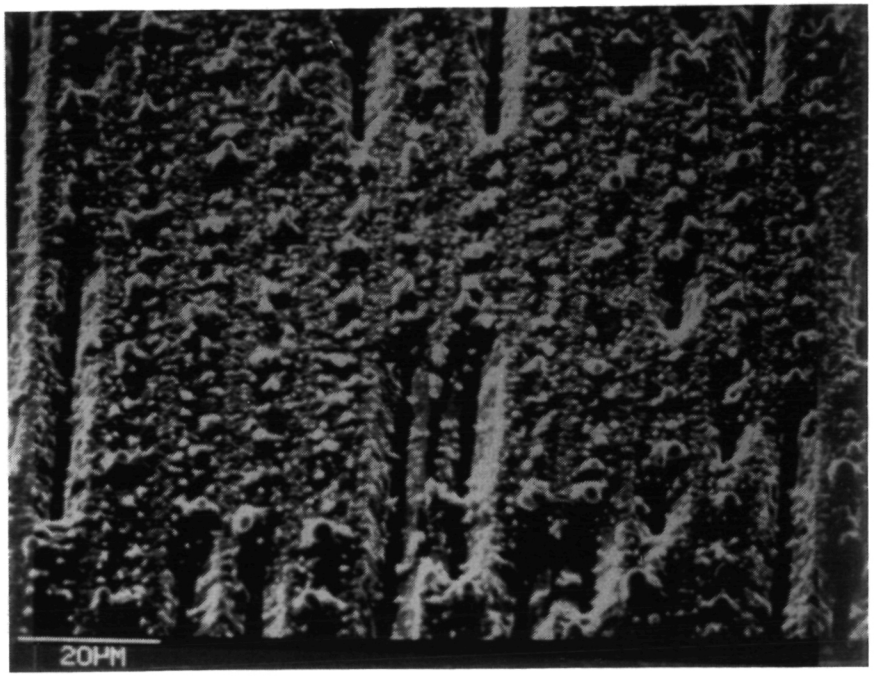


(b)

Figure 17. Continuous MOCVD growth on a 10 μm grating. (a) As-grown. (b) After laser scanning.

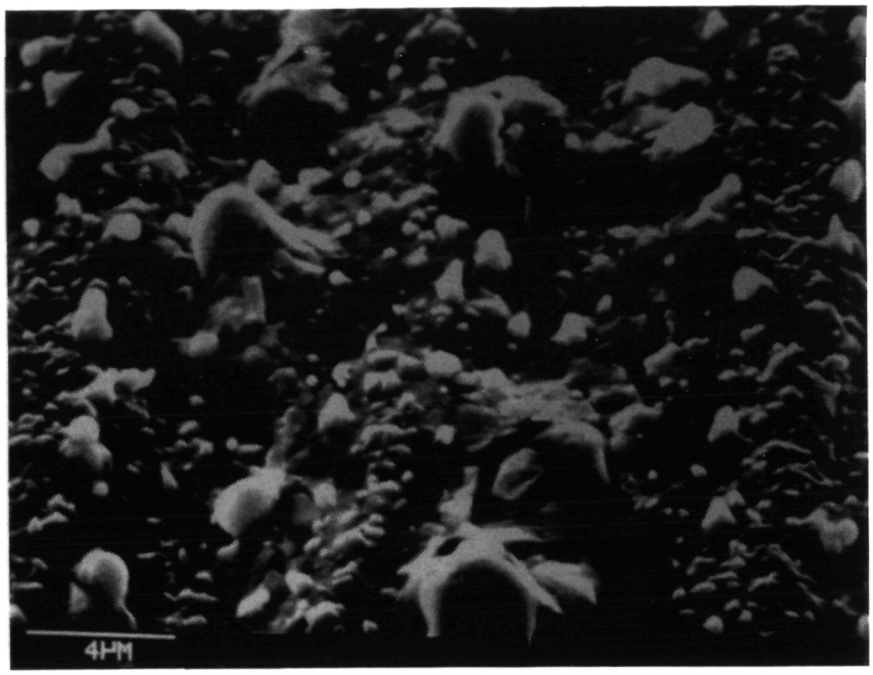


Figure 18. Close-up SEM view of recrystallized area from Figure 17b.

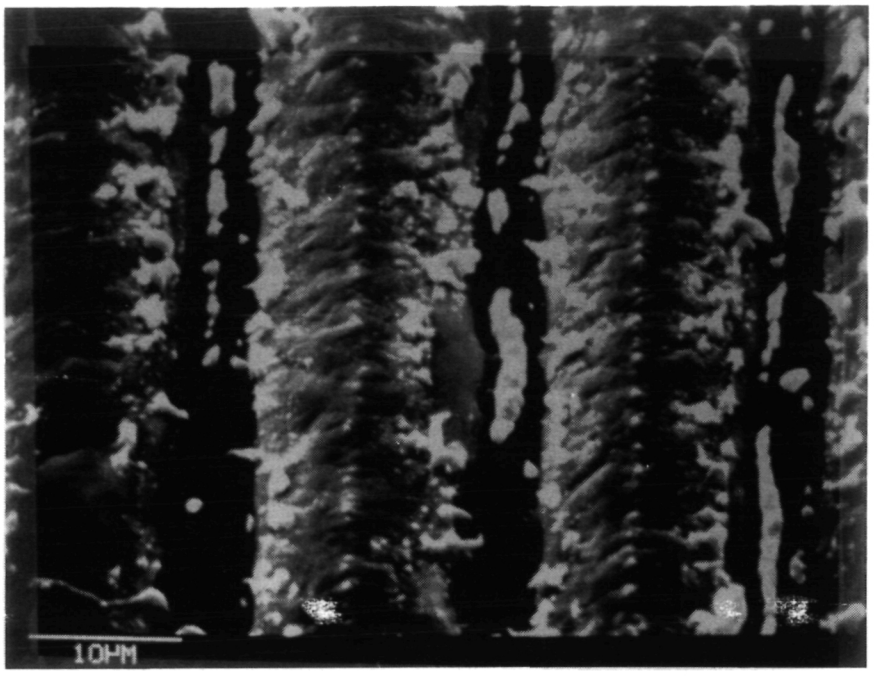


(a)

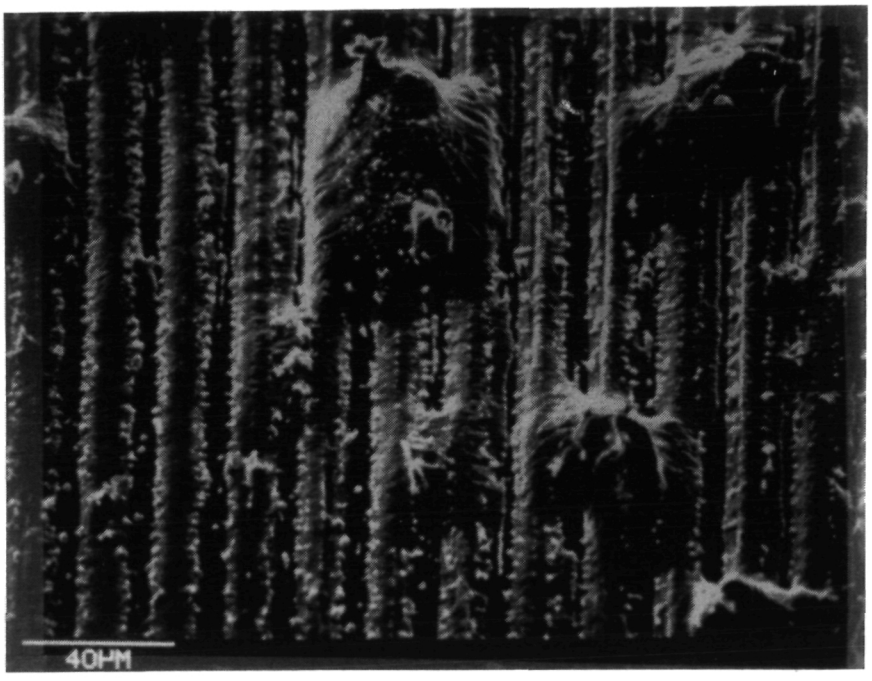


(b)

Figure 20. SEM micrographs of a 20 μm grating showing the results of laser scanning a continuous GaAs film. (a) Detail of the coverage over the grating lines. (b) View of areas where the GaAs has coalesced into droplet-shaped structures.

As one might expect, the 40 μm grating also demonstrated poor adhesion properties, even with a continuous as-grown GaAs film. An example of a recrystallized continuous as-grown film is shown in Figure 21. By increasing the scan speed about 6%, another specimen reveals the onset of recrystallization and illustrates that the melting begins at the edges of the grating lines (Figure 22).

## V. SUMMARY AND CONCLUSIONS

From the results of the laser recrystallization scans presented in the previous section, several important aspects of this type of graphoepitaxy have been determined. Of primary interest is the characteristic response of the GaAs films to the c.w. laser scan. We have found that within the range of scan speeds used (< 1.0 cm $s^{-1}$ to 5 cm $s^{-1}$), as limited by the available power from the Nd:YAG laser (~90 W maximum at the specimen surface), the observed recrystallization effects are limited. When the ratio of laser power to scan speed is below ≈20 W•s $cm^{-1}$ the GaAS film shows no structural change, as observed by scanning electron microscopy. At threshold the film begin to show signs of melting, especially at the corners of the grating lines. A slight increase in laser power ( or decrease in scan speed) produces complete melting and recrystallization of the film. As described previously, the appearance of the recrystallized film is strongly dependent on whether an underlying grating is present and also on the period of the grating. Because a lack of adhesion of the GaAs to the molybdenum substrate was a problem, the better adhesion characteristic of the smaller period gratings (10 μm and 5 μm) consistently produced more continuous recrystallized films than did the larger period gratings (20 μm amd 40 μm). Changing the laser power and scan speeds, while keeping the ratio of the two constant,

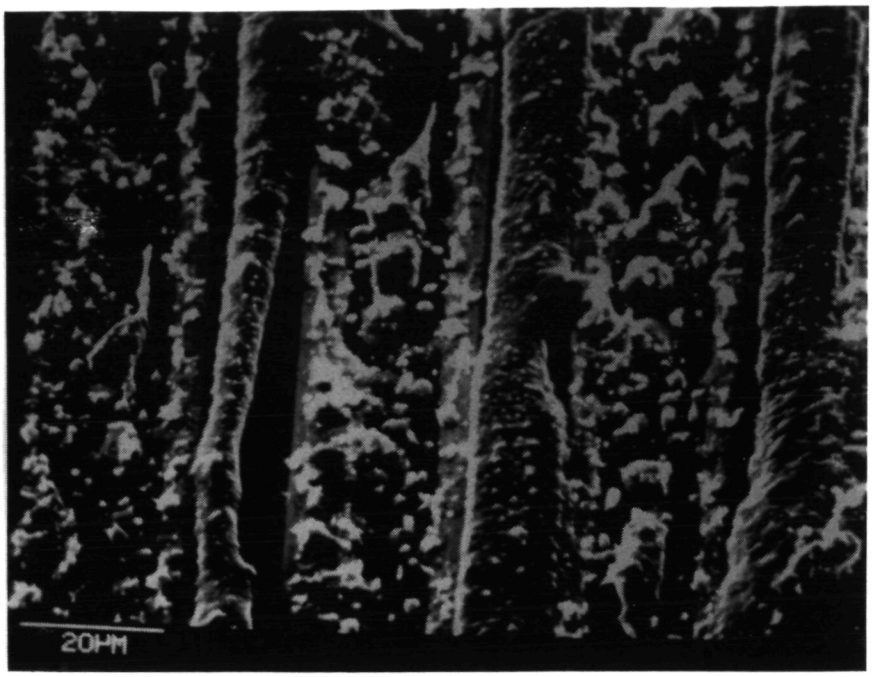


Figure 21. SEM micrograph of a recrystallized continuous GaAs films on a 40 μm grating.

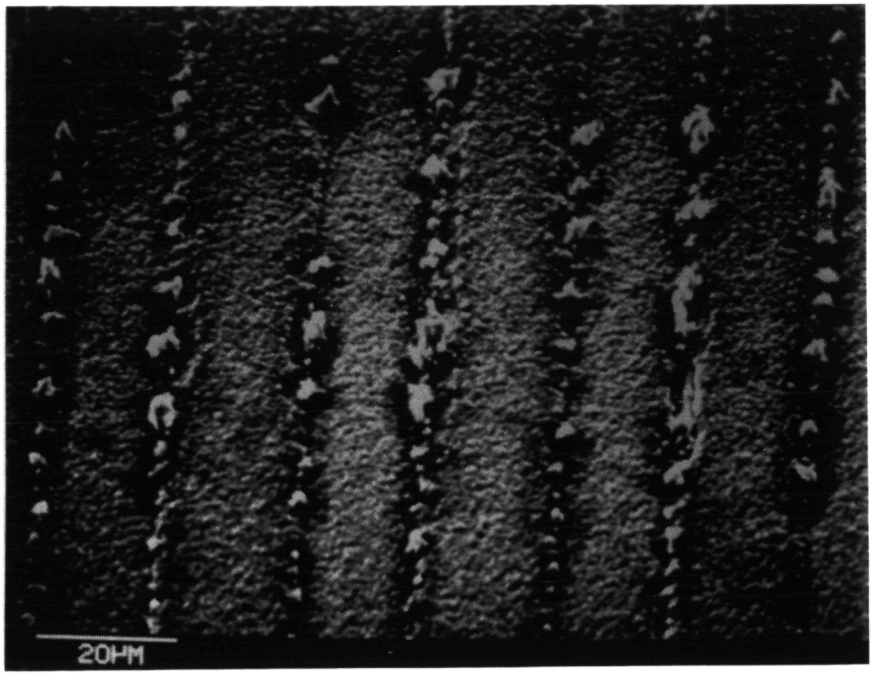


Figure 22. Onset of melting of the GaAs film on a 40 μm grating.

produced no apparent changes in the appearance of the recrystallized film. The only difference observed was that at higher laser power and scan speed the results were somewhat more consistent from one run to the next, and severe overheating of the film near the edges of the specimens was avoided. This effect is an indication of the thermal diffusion time associated with c.w. laser heating. A similar effect is the lack of sensitivity of the width of the recrystallized path to the degree of focussing of the laser spot on the specimen. When the beam was focussed to a 70 μm spot the width of the recrystallization path was ~ 500 μm. Defocussing to ~ 200 μm produced the same results. At higher scan speeds the path width narrowed somewhat but was still several times larger than the laser spot diameter. Clearly, the focussed light intensity is less important than the total power of the light spot within the range of parameters used. The relative slowness of this c.w. laser processing, as compared to pulsed techniques, for example, is responsible for the heat spreading out by conduction through the molybdenum and silicon substrate, resulting in a wide path of melted GaAs.

The general appearance of the recrystallized films can be described in two ways. First, with the larger period 40 μm and 20 μm gratings, the melted GaAs film invariably pulled out of the grating grooves and often "crawled" along the lines and coalesced into large droplet-shaped structures. This behavior occurred whether the as-grown GaAs film was continuous or not. The 10 μm period grating also demonstrated this tendency when the as-grown GaAs was discontinuous. Second, continuous recrystallized films were obtained with the smaller period 10 μm and 5 μm gratings. The as-grown GaAs on the 5 μm period gratings was always continuous and when these gratings and the 10 μm continuous film gratings were laser scanned, largely continuous

recrystallized films were obtained. Such films were considerably smoother than the as-grown material except for the appearance of small globular shapes which tended to lie along the grating lines. Except for these objects, the presence of the grating under the GaAs was difficult to discern. The question of whether these globs appeared as a result of arsenic loss is presently unanswered.

Comparison of the results obtained from laser scanning the different period grating substrates and the unpatterned substrates indicates that the presence of the small period grating is advantageous. Not only does the grating provide improved adhesion, but it also seems to have some effect on improving the crystallinity of the recrystallized film, as far as can be seen by scanning electron microscopy.

More study is clearly necessary to answer some of the questions which have arisen in the course of this work. First, since no difference in the appearance of the recrystallized films was observed whether arsine or nitrogen was used as a background gas, the degree to which the arsine prevented any arsenic loss should be determined by some method such as Auger microprobe. This technique should also indicate the composition of some of the interesting structures observed, such as the globular objects on the 5 μm gratings. Also, the crystalline nature of the recrystallized films remains unknown. X-ray diffraction analysis could give some indication of the degree of crystal orientation achieved by laser recrystallization of the 5 μm gratings. Further areas for investigation might also include improving the MOCVD growth techniques for obtaining better adhesion between the GaAs and the molybdenum. In fact, recent indications are that GaAs grows better on foreign substrates at considerably

higher temperatures than have previously been used (~900$^{o}$C as opposed to 650$^{o}$C). Experimentation with finer period gratings and different grating structures would also be of interest.

REFERENCES

1. M. W. Geis, D. C. Flanders, and Henry I. Smith, Appl. Phys. Lett. 35, 71 (1979).

2. K. T. Chan and J. M. Ballantyne, "Holographic Fabrication of Gratings in Metal Substrates," Annual Technical Report, NASA Research Grant NS 1651, November 1980 - October 1981.

3. Kenneth E. Bean, IEEE Trans. on Electron Devices ED-25, 1185 (1978).

4. Michel Josse and Don L. Kendall, Applied Optics 19, 72 (1980).

PUBLICATIONS LIST

Aspects of work supported by this program were reported in the following talks and publications:

1. "Device and Materials Research in the Cornell Submicron Facility," J. M. Ballantyne, Invited Seminar at Thompson CSF Research Lab, Orsay, France, October 1982.
2. "Monolithic Optoelectronics and MOCVD Growth," J. M. Ballantyne, Invited Seminar at IBM Yorktown Heights, August 1982.
3. "Some Examples of Microfabrication Techniques for Submicron Devices," J. M. Ballantyne, Invited paper presented at the International Conference on Microlithography - ME 82, Grenoble, France, October 5-8, 1982. Proceedings to be published.
4. "Characterization of High-Purity GaAs Grown by Low-Pressure OMVPE," J. R. Shealy, V. G. Kreismanis, D. K. Wagner, Z. Y. Zu, G. W. Wicks, W. J. Schaff, J. M. Ballantyne, L. F. Eastman, R. Griffiths, and G. E. Stillman, Proc. 1982 Symposium on GaAs and Related Compounds, September 19-22, 1982.
5. "Gallium Arsenide Materials for Applications in Solar Energy Conversion and Optical Communications," J. M. Ballantyne Seminar, Eastman Kodak Research Lab, Rochester, NY, January 26, 1981.

PERSONNEL INVOLVED IN THIS PROGRAM

J. M. Ballantyne, Professor

D. K. Wagner, Senior Research Associate

R. M. Fletcher, Graduate Research Assistant

K. T. Chan, Graduate Research Assistant

G. J. Sonek, Graduate Research Assistant

C. M. Harding, Research Support Specialist